ISSN 0029-3865

CBPF-NF-014/87

ORIGIN AND ORIENTATION OF ELECTRIC FIELD GRADIENT IN ORDERED FeNi

by

Diana Guenzburger and D.E. Ellis*

Centro Brasileiro de Pesquisas Físicas - CNPq/CBPF
Rua Dr. Xavier Sigaud, 150
22290 - Rio de Janeiro, RJ - Brasil

*Permanent address: Department of Physics and Astronomy
Northwestern University
Evanston, IL 60201, USA

ABSTRACT

The electronic structure of tetrataenite, the ordered phase of FeNi, has been studied in the molecular cluster approximation using local density theory. Clusters containing 13 and 19 atoms were embedded in the fcc host lattice and spin-unrestricted potentials were iterated to self-consistency. Local moments, magnetic hyperfine fields and electric field gradients (EFG) at the iron sites were determined for comparison with experiment. The orientation of the EFG principal axis is found to be parallel to the superstructure c-axis.

Key-words: Electric field gradient; FeNi; Alloys.

1 INTRODUCTION

Iron-nickel alloys Ni_xFe_{1-x} exist over the entire composition range[1-7] and, with various added elements such as Cr and C, are of considerable importance for structural applications where high strength and resistance to corrosion is required. Both bcc and fcc phases are found, with fcc disordered phases predominating for $x \geq 0.4$. Except for notable cases such as the ordered Ni_3Fe and NiFe structures, random occupancy of lattice sites by either type of atom is presumed. At low Ni concentrations, the fcc phase can be stabilized by quenching or phosphorous doping, and an antiferromagnetic structure is observed at low temperatures. The Invar alloys, famous for their low thermal expansion, span the anti- to ferro-magnetic transition region $0.25 \lesssim x \lesssim 0.35$.

The 50-50 composition forms an ordered compound with the CuAu structure, consisting of alternating layers of Ni and Fe on an fcc lattice. This superlattice compound is found in certain meteorites, and is known as tetrataenite[1,2]. It has also been obtained by neutron irradiation of the disordered FeNi alloy[3]. The disordered phase is most stable for $T_c \geq 590K$, and the diffusion rate for $T < T_c$ is very low. Observation of the relative fraction of tetrataenite in ferronickel meteorites permits useful estimates of the rate of cooling, of the order of 1-2K per million years. The ordered compound is resistant to corrosion, meteoritic samples in the form of lamellae being obtained by dissolving the host Fe-Ni matrix in acid.

A small tetragonal distortion of the fcc structure has been observed by X-ray diffraction[1]. Magnetic hyperfine fields (H_f) and electric field gradients (EFG) at Fe sites have been obtained by several groups, using Mössbauer spectroscopy[5-7]. In principle, the use of external magnetic fields in the Mössbauer experi-

ment permits determination of the *sign* of the EFG as well as its magnitude. In addition, the orientation of the principal EFG axis relative to the internal magnetic field direction can also be found. The present work was motivated in part by a desire to understand the origins of the observed EFG, and to resolve its orientation relative to that of the internal magnetic field. The sign of the theoretical EFG is determined unambiguously here, and related to the Ni-Fe vs Fe-Fe bonding interactions.

2 ELECTRONIC STRUCTURE CALCULATIONS

A. Theoretical Method

Local density selfconsistent field models of electronic structure have proved to be highly successful in describing properties of transition metals and intermetallic compounds. Both band structure and molecular cluster techniques have been developed as first principles tools using a linear combination of atomic orbitals (LCAO) variational approach[8] which is well suited to atomistic chemical interpretations of charge and spin densities as well as spectroscopic properties. Band structure methods and cluster models for a periodic system tend to the same limit as the cluster size increases, and evidence has gradually accumulated that 3-4 shells of neighbors is sufficient to represent most properties of a particular atomic environment. In treating alloy properties, where local order may be a dominant factor rather than long-range periodicity, representation of the system by small embedded clusters is not only computationally attractive but also physically reasonable.

We have calculated the electronic structure of clusters representing the 50-50 FeNi ordered alloy. We considered both a 13-atom cluster and a 19-atom cluster (Fig. 1), the latter to explore the effect of cluster size. In the mineral tetrataenite[1,2], which has CuAu structure, each Fe atom is surrounded by 8 Ni and 4 Fe nearest neighbors (NN), with local symmetry D_{4h}, as seen in Fig. 1. The second shell of neighbors (NNN), included in the 19 atom cluster, is made up of 6 Fe atoms, forming an octahedron around the Fe atom at the center of the cluster. In Table 1 are given the interatomic distances used in the calculations.

The electronic structure for these clusters was obtained with the Discrete Variational (DV) method[8] in the local exchange approximation[9]. Self-consistent one-electron wave functions were derived by solving approximately the equation

$$(h_\sigma - \varepsilon_{i\sigma})\phi_{i\sigma} = [-\frac{\nabla^2}{2} + V_{coul} + V_x^\sigma - \varepsilon_{i\sigma}]\phi_{i\sigma} = 0 \qquad (1)$$

where the one-electron Hamiltonian (in Hartree atomic units) consists of a kinetic energy term, a Coulomb potential energy term which includes electron-nuclei and electron-electron interactions, and an exchange term which may be expressed as:

$$V_x^\sigma(\vec{r}) = -3\alpha[\frac{3}{4\pi}\rho_\sigma]^{1/3} \qquad (2)$$

and may be different for each spin σ. V_x^σ is thus a function of the electronic spin density $\rho_\sigma(\vec{r})$ defined as

$$\rho_\sigma(\vec{r}) = \sum_i n_{i\sigma}|\phi_{i\sigma}(\vec{r})|^2 \qquad (3)$$

and $\alpha=2/3$[9]. Here $n_{i\sigma}$ is the occupation of spin orbital $\phi_{i\sigma}$.

The cluster molecular orbitals ϕ_i are expanded over a basis of numerical atomic orbitals, which may include both occupied and vacant orbitals for greater variational freedom. One then obtains a set of secular equations

$$([H] - [E]\,[S])\,[C] = 0 \tag{4}$$

where [C] is the matrix of the coefficients of the expansion, and [H] and [S] are the energy and overlap matrixes, respectively. In the DV method, all the matrix elements in Eq. (4) are calculated by numerical integration; in the valence region, the pseudo-random diophantine integration method[8] is used, and in the core region a precise polynomial integration is performed[10], which is essential for the accurate evaluation of hyperfine interactions.

In order to better represent the solid by the clusters, these are "embedded" in the potential field of several shells of surrounding atoms[11]. The core-region potential of each exterior atom is truncated, to simulate Pauli exclusion effects.

The quadrupole splitting Δ_{EQ} of the I = 3/2 nuclear gamma resonance line of ^{57}Fe, when an internal magnetic field is present, may be expressed as[12]

$$\Delta_{EQ} = \frac{1}{2}\, eV_{zz}Q\left(\frac{3\cos^2\theta-1}{2}\right) \tag{5}$$

where θ is the angle between the direction of the magnetic field and the principal axis of the field gradient. θ cannot be determined from a single Mössbauer experiment, an independent measurement being necessary. On the other hand, one may calculate the

principal component of the field gradient tensor V_{zz} using the expression[12] (in a.u.):

$$V_{zz} = \sum_k Z_k \frac{3z_k^2 - r_k^2}{r_k^5} - \sum_{i,\sigma}^{*} n_{i\sigma} \langle \phi_{i\sigma} | \frac{3z^2 - r^2}{r^5} | \phi_{i\sigma} \rangle \qquad (6)$$

where the first term represents the contribution of the surrounding nuclei of atomic number Z_k (or the nuclei shielded by the core electrons, in the case of a "frozen core" approximation). The second term is the electronic contribution, and represents a sum over the contributions of occupied spin orbitals $\phi_{i\sigma}$, with occupation $n_{i\sigma}$.

When the spin orbitals in the second term of Eq. (6) are expanded in the linear combination of atomic orbitals, one-center and multiple-center terms result. The first are calculated analytically, using the coefficients of Eq. (4), and the latter are evaluated using special techniques of numerical integration[13,14].

B. Quadrupole Splitting of ^{57}Fe in FeNi

In Table II are given the calculated values of the components of V_{zz} of the Fe atom at the center of the clusters, as well as its total value. *It is seen that the calculated V_{zz} is positive.* This result indicates that $\theta=0$ (and not $\theta=90^0$), that is, the axis of V_{zz} is parallel to the axis of the internal magnetic field, since the measured Δ_{EQ} is also positive. This also implies that the internal magnetic field is oriented perpendicular to the lamallae; i.e., along the z-axis of Fig. 1. The quadrupole moment Q of ^{57}Fe in the excited state I=3/2 has been estimated to be of the order of +0.2[12,15]. Eq. (5) now reduces to:

$$\Delta_{EQ} = \frac{1}{2} V_{zz} \; e \; Q \qquad (7)$$

since the angular term in brackets is equal to +1 for $\theta=0$.

Of all the contributions given in Table II, it can be seen that it is the one-center spin down term that determines the sign and, to a great extent, the magnitude of V_{zz}. The nuclear and multiple-center terms are all very small, and the one-center spin ↑ adds to a small number also, since the spin ↑ valence states at the site of the central Fe atom are all occupied (see the density of states diagrams, Figs. 2 and 3).

From the results given in Table II it is also seen that increasing the number of atoms in the cluster from 13 to 19 does not have a major effect on V_{zz}; this increases our confidence in the stability of the results regarding cluster size.

To better understand the origin of the positive contribution to V_{zz} given by the spin ↓ orbitals, we have broken up this contribution into its components according to the symmetry group D_{4h}. These are given in Table III.

On examining these numbers, it may be noticed that the a_{1g} orbitals give a contribution which is negative, and of about the same magnitude as the b_{1g}. For the central Fe atom, the $3d_{z^2}$ orbital transforms as a_{1g}, and is pointed along the z axis, towards two of the Fe atoms in the second shell of neighbors. The $3d_{x^2-y^2}$ transforms as b_{1g}, and points, in the x and y directions, also towards Fe atoms in the second shell of neighbors. The contributions of these two orbitals almost cancel each other. As seen in Table IV, the six Fe atoms in this shell are almost equivalent, from the point of view of chemical environment; in fact, the Mulliken populations of the orbitals of the axial and equatorial next nearest

neighbor Fe atoms are very similar. This explains the almost null one-center contribution to V_{zz} coming from the $3d_{z^2}$ and $3d_{x^2-y^2}$ pair of the central Fe.

The orbitals $3d_{xy}$, $3d_{xz}$, and $3d_{yz}$ of central Fe, which are degenerate in octahedral or cubic symmetries, decompose into $b_{2g}(3d_{xy})$ and $e_g(3d_{xz}, 3d_{yz})$ in D_{4h} symmetry. The b_{2g} orbital gives a large positive contribution to V_{zz}, which is only cancelled in part by the negative contribution of the e_g pair. The explanation for this lies again in the electronic environment which the electrons in these orbitals experience. The $3d_{xy}$ orbital points towards the 4 Fe atoms in the xy plane. On the other hand, the $3d_{xz}$ and $3d_{yz}$ point toward the Ni atoms. These last withdraw a small amount of charge from the Fe atoms, as seen in Table IV. In fact, estimates of electronegativity values[16] show that Ni attracts electronic charge in a metallic bond more than Fe does. This explains the reduction of the one-center spin $\uparrow$ contribution to V_{zz} due to the e_g orbitals. The resulting V_{zz} due to all 3d orbitals is thus positive. We also give in Table III the contributions of the 4p orbitals. These are seen to be small, and largely cancel one another.

To have additional proof for the origin of the positive V_{zz}, we have made a calculation for a cluster in which the Ni atoms above the central plane in Fig. 1 have been substituted by Fe atoms, and the 4 Fe atoms surrounding the central atom in the x-y plane were in turn replaced by Ni. The resulting V_{zz} which was obtained was *negative* (-0.23 a.u.), showing that indeed the position of the Ni atoms in the ordered FeNi alloy, to which point the $3d_{xz}$ and $3d_{yz}$ orbitals of the Fe atoms, is what determines the sign of V_{zz}.

In summary, the sign that we obtained for V_{zz} is coherent with what may be expected from considerations of the bonding between each Fe atom and its neighbors.

C. Magnetic Properties

In Table IV are given the Mulliken populations of the atoms in the cluster, as well as the charges and magnetic moments. In these spin-polarized calculations, the difference between the spin ↑ and spin ↓ total populations on a given atom may be used to define the local magnetic moment in Bohr magnetons.

We notice in Table IV that all atoms have increased 3d populations, as compared to the free atom configuration. This result is consistent with band structure and cluster calculations for a variety of transition metals and their alloys. The 4s population is decreased, and some 4p charge appears. Overall, the NNN atoms present more atomic-like character than the central atom, which, by its position in the cluster, represents better a bulk atom[14,17]. The rather large positive charge on the central atom is essentially a cluster effect; the population analysis accentuates the special role of the basis attached to the central atom. A volume integration generally yields smaller charge differences, due to the different allocation of diffuse charge. In fact, the finite groups of atoms considered to represent the solid show an inbalance of the charge distribution among similar atoms, due to truncation of the external atoms bonds.

The calculated magnetic moments on the Fe atoms are considerably larger than the experimental value of bulk Fe. Cluster calculations for Fe metal with the DV method[14] give a moment of $2.8\mu_B$, which is somewhat larger than the experimental value of $2.2\mu_B$ but still considerably smaller than the presently calculated value. Again, the increased moment on the NNN Fe atoms is due to the fact that these are surface atoms in the cluster and thus only partially bonded. The moments on

the Ni atoms are somewhat higher than that for Ni metal. We conclude that the partial isolation of the Fe atoms, stacked as two-dimensional arrays, is the factor responsible for the increased magnetic moment of Fe atoms in FeNi, as compared to bulk iron.

We have calculated the contact hyperfine field at the nucleus of the central Fe atom, in the manner that follows: the spin density of the valence electrons was obtained from the cluster calculation, and the 1s, 2s and 3s spin densities were obtained from an atomic local density calculation for the same value of α. The hyperfine field is large and negative (-244 kOe); the valence contribution is positive (+164 kOe) and more than cancelled by the negative terms of the core polarization. The theoretical value is in very good agreement with the value reported for meteoritic tetrataenite (288 kOe) and microcrystalline material produced by neutron irradiation (288 kOe, 327 kOe). The magnetic properties of several Fe-Ni alloys have been investigated in another work[18]. From general experience, we conclude that the present calculated value of H_f is uncertain by ±50kOe due to our approximate treatment of core contributions and fundamental limitations of the local density theory used here.

ACKNOWLEDGEMENTS

This work was supported by the CNPq (Brasil) and by the U.S. National Science Foundation, Grant no. INT83-12863. The authors thank Prof. Jacques Danon for interesting discussions.

REFERENCES

1. R.S. Clarke, Jr. and E.R.D. Scott, American Mineralogist, 65, 624 (1980).
2. J.F. Albertsen, Physica Scripta 23, 301 (1981).
3. J. Paulevé, D. Dautreppe, J. Laugier and L. Néel, C.R. Acad. Sci. Paris 254, 965 (1962).
4. A.D. Romig, Jr. and J.I. Goldstein, Met. Trans. A11, 1151 (1980); C.E. Johnson, M.S. Ridout and T.E. Cranshaw, Proc. Phys. Soc. 81, 1079 (1963); U. Gonser, S. Nasu and W. Kappes, J. Magn. Mag. Mat. 10, 244 (1979).
5. Y. Gros and J. Paulevé, J. Physique 31, 459 (1970).
6. J. Danon, R.B. Scorzelli, I. Souza Azevedo, J. Laugier and A. Chamberod, Nature 284, 537 (1980).
7. R.B. Scorzelli, Ph.D. Thesis, Univ. of Paris, 1985 (unpublished).
8. D.E. Ellis, Int. J. Quant. Chem. S2, 35 (1968); D.E. Ellis and G.S. Painter, Phys. Rev. B2, 2887 (1970); A. Rosén, D.E. Ellis, H. Adachi, and F.W. Averill, J. Chem. Phys. 85, 3629 (1976).
9. J.C. Slater, "The Self-Consistent Field for Molecules and Solids", Vol. 4 of *Quantum Theory of Molecules and Solids*, McGraw-Hill, New York (1974).
10. A.H. Stroud, *Approximate Calculation of Multiple Integrals*, Prentice-Hall, Englewood Cliffs, New Jersey (1971).
11. G.A. Benesh and D.E. Ellis, Phys. Rev. B24, 1603 (1981).
12. N.N. Greenwood and T.C. Gibb, *Mössbauer Spectroscopy*, Chapman and Hall, London (1971).
13. D. Guenzburger and D.E. Ellis, Phys. Rev. B22, 4203 (1980).
14. D. Guenzburger and D.E. Ellis, Phys. Rev. B31, 93 (1985).
15. S.N. Ray and T.P. Das, Phys. Rev. B16, 4794 (1977).
16. R.E. Watson and L.H. Bennett, Phys. Rev. B18, 6439 (1978).
17. D.E. Ellis and D. Guenzburger, Phys. Rev. B31, 1514 (1985).
18. D. Guenzburger, D.E. Ellis and J. Danon, J. Mag. Magn. Mat. 59, 189 (1986).

TABLE I. Interatomic distances in FeNi ordered phase (Ref. 1).

	Bond Distance (Å)
Fe-Fe (1st neighbor)	2.53
Fe-Ni	2.53
Fe-Fe (2nd neighbor)	3.58

TABLE II. Calculated value of V_{zz} and its components (in a.u.).

nuclear: +0.073

	13 atom cluster	19 atom cluster
1-center ↑	+0.026	+0.149
1-center ↓	+0.350	+0.407
2,3-center ↑	+0.012	+0.013
2,3-center ↓	+0.012	+0.010
Total V_{zz}	+0.473	+0.652
Δ_{EQ} (mm/s) [a]	+0.74	+1.03

(a) According to Eq. (7). Value of Q from Ref. (15) (Q=0.156b).

TABLE III. One-center spin-down contributions to V_{zz} (in a.u.).

(19-atom cluster)

3d	$a_{1g}(3d_{z^2})$	: -0.680
	$b_{1g}(3d_{x^2-y^2})$	: +0.681
	$b_{2g}(3d_{xy})$	: +1.005
	$e_g(3d_{xz}+3d_{yz})$	: -0.646
4p	$a_{2u}(4p_z)$	: -0.120
	$e_u(4p_x+4p_y)$	: +0.171

TABLE IV. Mulliken populations and charges for the 19 atom cluster. NN=nearest neighbor; NNN=next nearest neighbor

	Fe (center)	Fe_{NN}	Ni	Fe_{NNN} (axial)	Fe_{NNN} (equatorial)
3d	6.68	6.60	8.70	6.45	6.48
4s	0.50	0.75	0.83	0.97	1.08
4p	0.40	0.59	0.60	0.52	0.43
charge	0.43	0.06	-0.12	0.06	0.01
magnetic moment (μ_B)	3.33	3.40	0.79	3.98	3.76

FIGURE CAPTIONS

Fig. 1 - 19 atom cluster representing the FeNi 50-50 alloy.

Fig. 2 - 3d, 4s and 4p density of states at the central Fe atom for spin ↑.

Fig. 3 - 3d, 4s and 4p density of states at the central Fe atom for spin ↓.

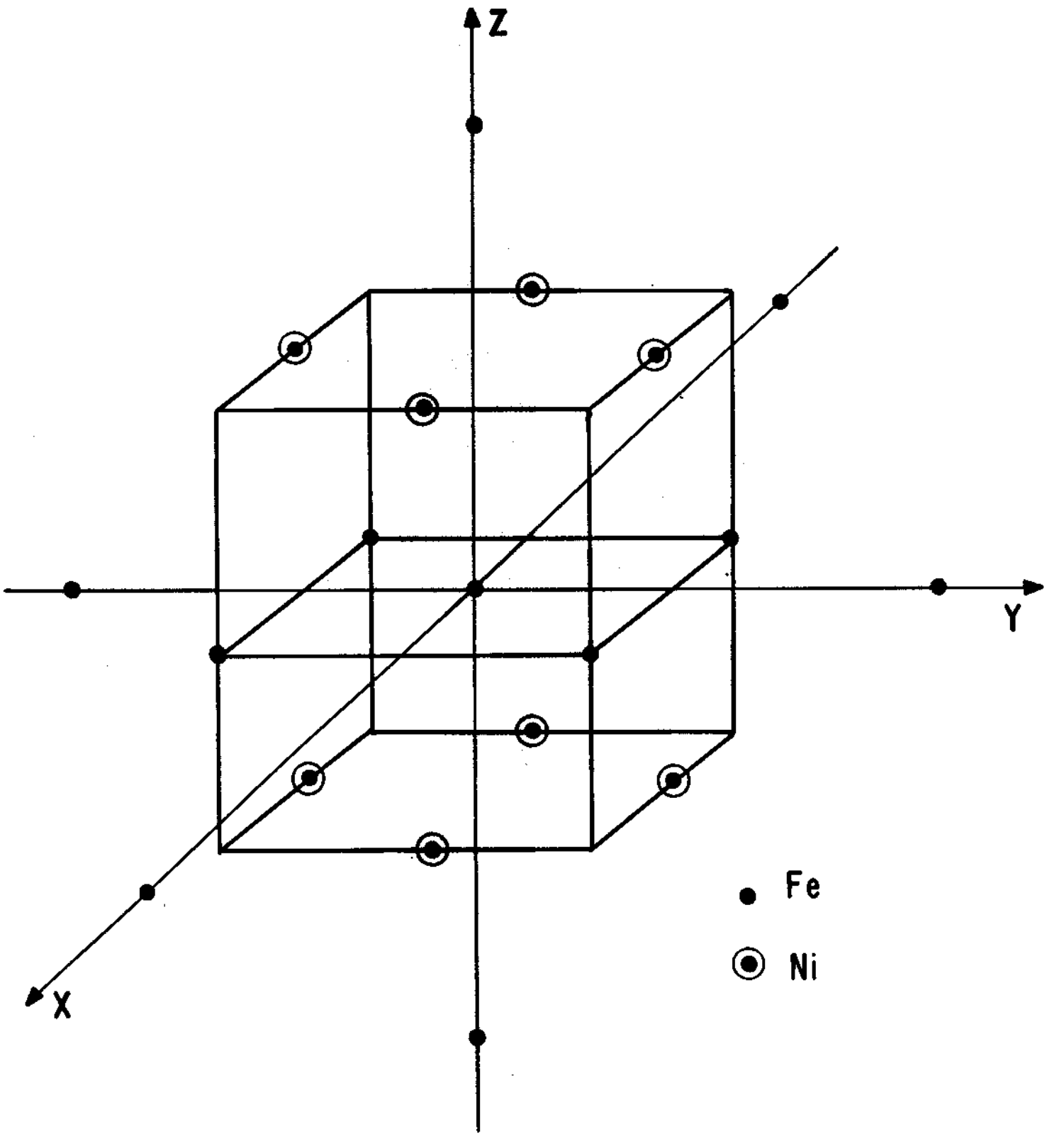

FIG.1

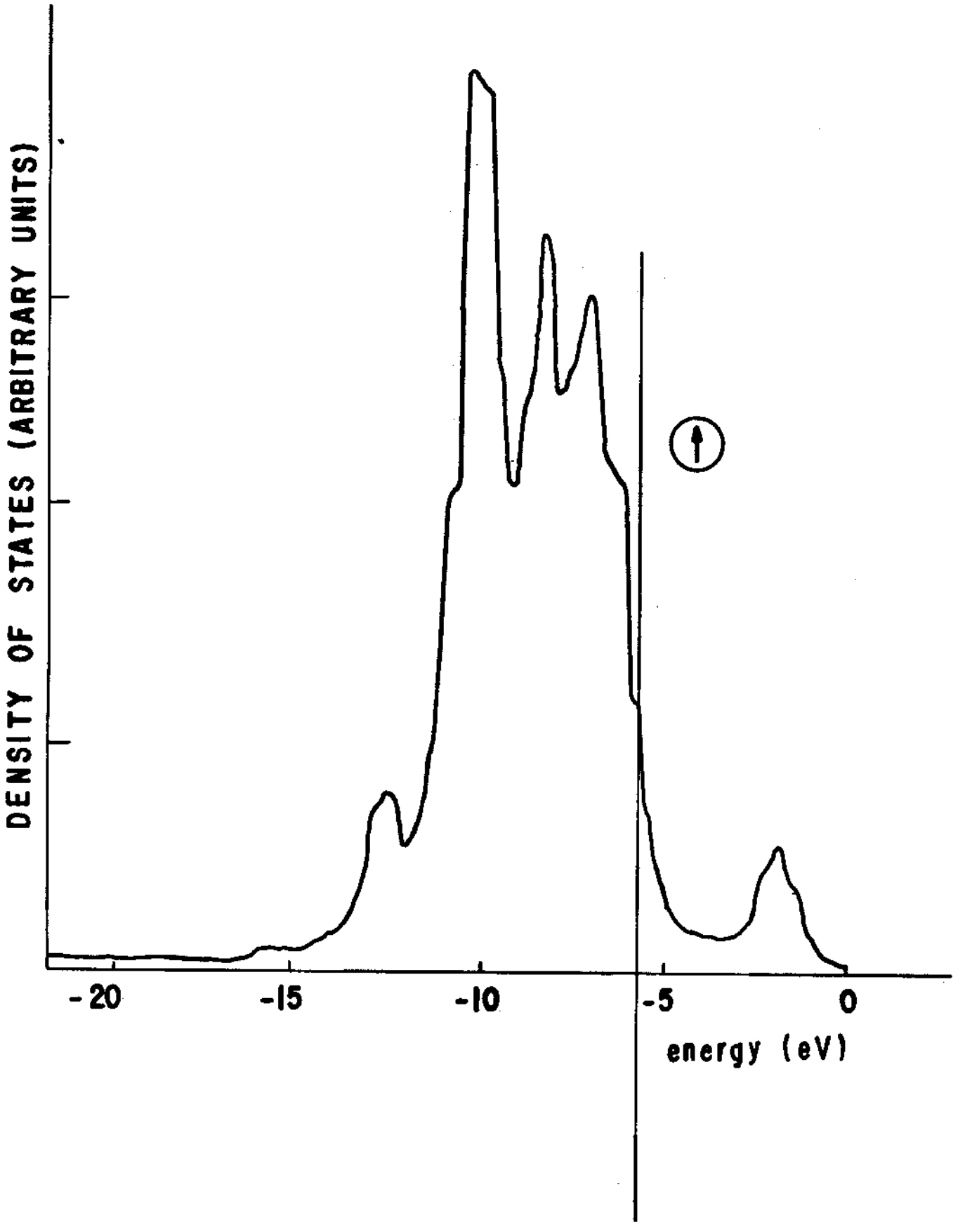

Fig. 2

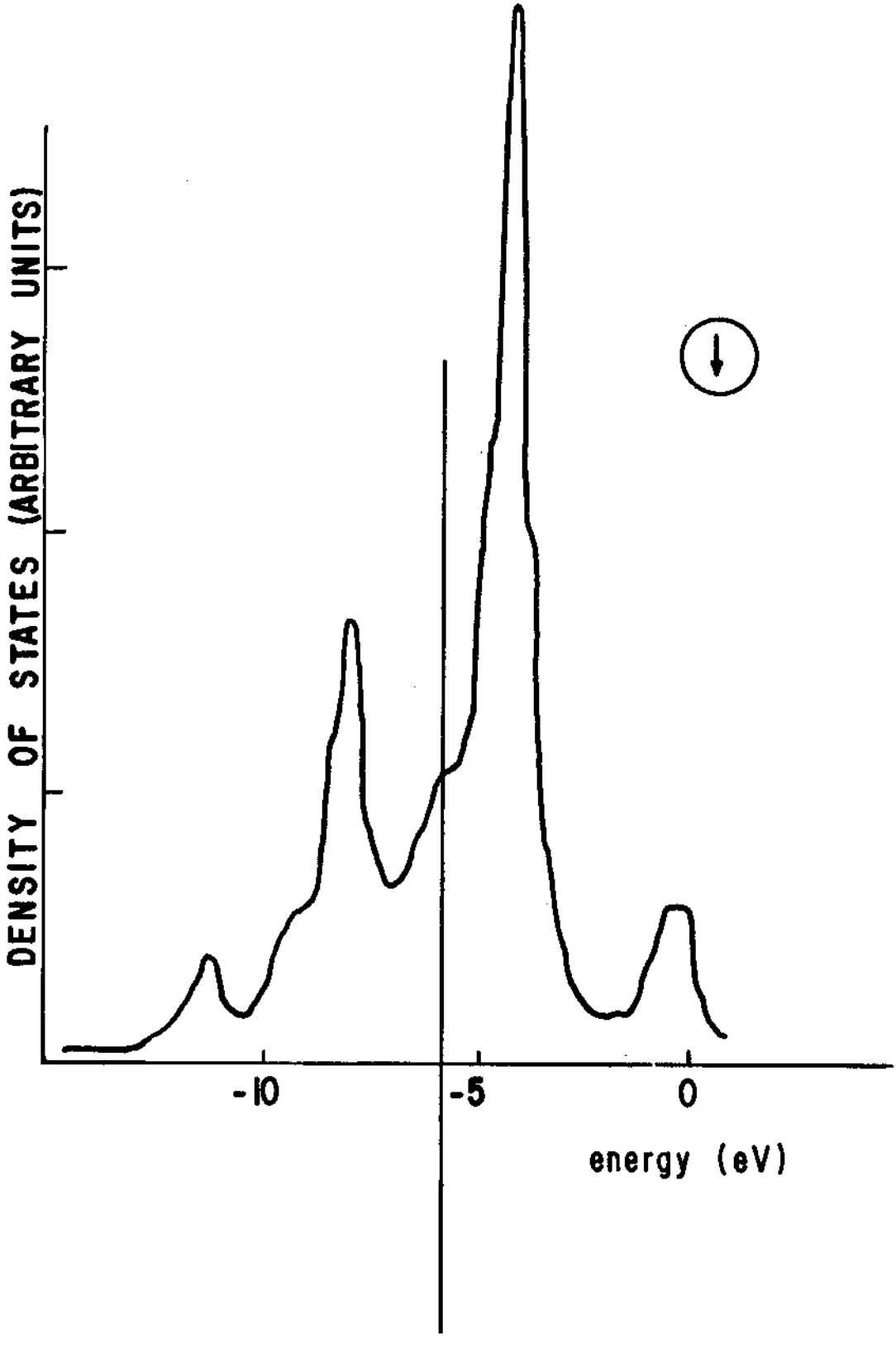

Fig. 3